OXFORD

SOT | Society of Toxicology
academic.oup.com/toxsci

TOXICOLOGICAL SCIENCES, 181(1), 2021, 105–114

doi: 10.1093/toxsci/kfab017
Advance Access Publication Date: 9 February 2021
Research Article

A Single Microbiome Gene Alters Murine Susceptibility to Acute Arsenic Exposure

Qian Wang,* Timothy R. McDermott,†,1 and Seth T. Walk*,1

*Department of Microbiology and Immunology, Montana State University, Bozeman, Montana 59717; and †Department of Land Resources and Environmental Sciences, Montana State University, Bozeman, Montana 59717

[1]To whom correspondence should be addressed. Department of Land Resources and Environmental Sciences, 334 Leon Johnson Hall, P.O. Box 173120, Bozeman, MT 59717. E-mail: timmcder@montana.edu and Department of Microbiology and Immunology, 109 Lewis Hall, PO Box 173520, Bozeman, MT 59717. E-mail: seth.walk@montana.edu

ABSTRACT

Environmental toxicant exposure contributes to morbidity and mortality of many human diseases. With respect to arsenic, microbially driven chemical transformations dictate its toxicity and mobility in virtually every environment yet studied, so a general hypothesis is that the human gut microbiome determines disease outcome following exposure. However, the complex nature of the gut microbiome and the myriad of potential interactions with human cells/tissues make it challenging to quantify the influence of specific arsenic-active functions—a requisite step in developing effective disease prevention and/or clinical intervention strategies. To control both mammalian and microbial function during toxicant exposure, we genetically defined the gut microbiome of mice using only *Escherichia coli* strain, AW3110 (△*arsRBC*), or the same strain carrying a single genome copy of the *Fucus vesiculosus* metallothionein gene (AW3110::*fmt*); a cysteine-rich peptide that complexes with arsenite, facilitating bioaccumulation and reducing its toxic effects. AW3110::*fmt* bioaccumulated significantly more arsenic and gnotobiotic mice colonized by this strain excreted significantly more arsenic in stool and accumulated significantly less arsenic in organs. Moreover, AW3110::*fmt* gnotobiotic mice were protected from acute toxicity exposure (20 ppm As^{III}) relative to controls. This study demonstrates—in a highly controlled fashion—that a single microbiome function (arsenic bioaccumulation) encoded by a single gene in a single human gut microbiome bacterium significantly alters mammalian host arsenic exposure. The experimental model described herein allows for a highly controlled and directed assessment of microbiome functions, and is useful to quantify the influence of specific microbiome-arsenic interactions that help mitigate human disease.

Key words: arsenic; microbiome; bioaccumulation; host exposure.

Arsenic ranks first on the United States Environmental Protection Agency Priority List of Hazardous Substances (Astdr, 2019), impacting the drinking water of over 200 million people worldwide (Bhattacharjee *et al.*, 2013; Naujokas *et al.*, 2013). Chronic arsenic exposure increases both the onset and the progression of several human diseases, collectively referred to as arsenicosis, including lung, skin, bladder, and liver cancers (Faita *et al.*, 2013; Liu *et al.*, 2008). Interestingly, susceptibility to arsenicosis varies between similarly exposed individuals (Cubadda *et al.*, 2015; Naujokas *et al.*, 2013), suggesting factors in addition to toxicant exposure govern disease. Host genetics, age, gender, and diet no doubt influence exposure outcomes, and given the highly personal nature of the gut microbiome (i.e., large inter-individual variability), the microbial composition of the gut likewise holds the potential to play a relatively large role during and after exposure to environmental toxicants (Coryell *et al.*, 2019; McDermott *et al.*, 2020).

Chemical transformation of arsenic by microbes greatly influences its toxicity and mobility in all environments thus far studied (Oremland and Stolz, 2003, 2005; Stolz and Oremland,

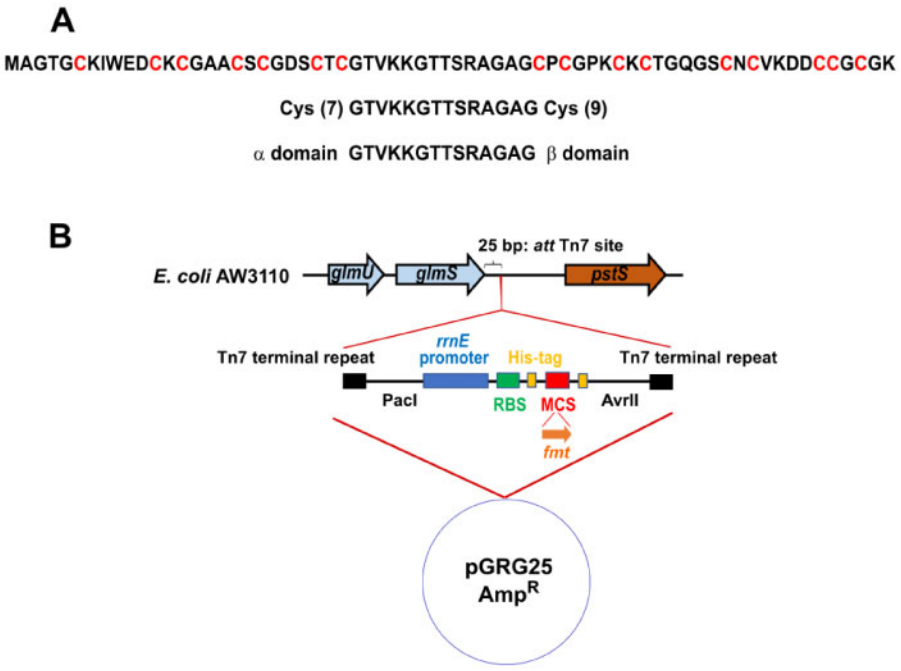

Figure 1. Structure of the insertion *fmt* construct and Fmt peptide. (A) Fmt amino acid sequence displaying β and α domains containing 7 and 9 Cys residues, respectively, that flank the 14 amino acid linker. (B) The synthesized *rrnE* promoter, RBS and *fmt*-flanking His-tags introduced via pGRG25 to the conserved chromosome Tn7 insertion site in strain AW3110.

1999) and for this reason, the same expectation should hold for the human gut ecosystem. We recently showed that both perturbation (i.e., antibiotic treatment) and/or removal of the murine microbiome (i.e., germ-free status) increases arsenic toxicity (Coryell *et al.*, 2018), but evidence that individual microbiome members influence arsenic exposure is lacking. Moreover, no study has provided direct evidence that any one microorganism or specific microbial function in the mammalian gut either diminishes or exacerbates host disease during arsenic exposure.

In general, microbes transform arsenic for detoxification/resistance or to generate energy. Common transformations include arsenic oxidation, reduction, (de)methylation, cellular extrusion, and bioaccumulation (i.e., complexing with cellular components) (McDermott *et al.*, 2020; Oremland and Stolz, 2003; Stolz *et al.*, 2006). Such activities vary greatly among microbial species and even at the strain level in terms of presence-absence and efficiency. When viewed in the context of well documented gut microbiome heterogeneity (Martinson and Walk, 2020) and the variety of ways that gut microbiome members influence the host (e.g., liver function, immunity, cognition, and overall physiologic processes), it becomes a reasonably complex exercise to quantify the influence of a single member of the mammalian gut during any toxicant exposure. In this study, we leverage microbial genetics and a germ-free mouse model to tightly control arsenic transformations by both the mammalian host (cannot methylate arsenic—a primary mammalian detox mechanism) and the gut microbiome (production of metallothionein only; no arsenate reductase nor active arsenite extrusion). Previous work suggested that arsenic bioaccumulation is an important microbiome function during arsenic exposure via drinking water (Coryell *et al.*, 2018). Here, we provide the first direct evidence that indeed a single arsenic-active molecule (metallothionein) produced by a single common human gut microbiome species (*Escherichia coli*) provides significant protective benefit to a mammalian host during arsenic exposure. Our results provide strong support for the use of microbiome customization to mitigate arsenicosis and other exposure-related pathologies.

MATERIALS AND METHODS

Bacterial Strains, Genes, and Genetic Modifications. *E. coli* strain AW3110 has been described previously (Carlin *et al.*, 1995). Briefly, it is derived from the wild type stain W3110 (Coli Genetic Stock Center) that does not naturally carry the *arsM* gene and the complete *arsRBC* operon was experimentally deleted (Carlin *et al.*, 1995). As such, it is incapable of arsenite (As^{III}) methylation via ArsM, arsenate (As^{V}) reduction to As^{III} via ArsC, nor trafficking via ArsB (As^{III} extrusion). The *Fucus vesiculosus* metallothionein gene (*fmt*) (Morris *et al.*, 1999) was synthesized commercially (Biomatik) and received within pET29a+ (Novagen). The synthesized construct also included the *rrnE* promoter to facilitate constitutive expression (Maeda *et al.*, 2015), a ribosome binding site, and two flanking His-tags to facilitate dot blot analysis of the expressed peptide using anti-His antibodies (Figure 1). Further molecular manipulation and plasmid construction were conducted at Montana State University. The synthesized fragment was subcloned as a PacI-AvrII restriction fragment into pGRG25, which facilitated convenient, markerless insertion of transgenes into the AW3110 chromosome followed by incubation at non-permissive temperatures (42°C) to eliminate the delivery plasmid and finally generate AW3110::*fmt* (McKenzie and Craig, 2006).

Quantification of Growth and Bioaccumulation. Characterizations of AW3110 and AW3110::*fmt* growth responses to inorganic As^{III} (as sodium arsenite) were conducted in LB broth containing varying concentrations of As^{III}. Growth was quantified as optical density (OD_{595}) using a SpectraMax microtiter plate reader

(Molecular Devices, California), and by viable cell counts determined by serially diluting cultures or homogenized stool samples, spread onto LB agar, and then counted after overnight incubation at 37°C. Viable cell counts were normalized on a media volume (mL) or stool dry weight basis (oven dehydration).

For quantification of arsenic bioaccumulation, cells were grown to stationary phase in LB, collected via centrifugation (8000 × g), washed 3× in Tris-HCl buffer (20 mM, pH 7.2), and resuspended in Tris-HCl buffer (20 mM, pH 7.2) containing different concentrations of As^{III} at 37°C. After 2 hours of incubation, cells were collected by centrifugation (8000 × g), washed 3× in Tris-HCl buffer (20 mM, pH 7.2), and finally digested in 5% trace metal grade nitric acid using heat and pressure (115°C, 29.7 PSI for 30 min) (Coryell *et al.*, 2018).

Evaluation of Phosphate Stress Response. Induction of alkaline phosphatase (AP), the native reporter enzyme for the phosphate stress response (PSR) was determined. *E. coli* were first grown to saturation in modified M9 media (Sambrook, 2001), containing reduced potassium phosphate (100 μM) and buffered with 20 mM 3-(N-morpholino) propanesulfonic acid, pH 7.2. Cells were collected by centrifugation, washed 3× in 50 mM Tris-Cl (pH 8.0), and suspended in the same buffer containing 0.12 mM p-nitrophenylphosphate, a chromogenic AP substrate. Monitoring of AP activity used methods we have previously described (Botero *et al.*, 2000).

In Vitro Competition Experiments. *E. coli* AW3110 and AW3110::*fmt* were inoculated equally into LB with or without the addition of 50 μM As^{III}. Co-cultures were sampled daily and bulk DNA was extracted from the cell pellets using an Easy-DNA kit (Invitrogen, Carlsbad). Quantitative PCR was then performed using AzuraQuant Green Fast qPCR Master Mix (Azura Genomics Inc.) with primers listed in Supplementary Table 1 that differentiated between the two competing strains. qPCRs were performed in triplicate using a LightCycler 96 thermocycler (Roche) with the following conditions: 95°C for 10 min, followed by 40 cycles of 95°C for 15 s and 55°C for 30 s, followed by a hold at 4°C. Standard curves were generated to estimate cell numbers based on observed Ct values.

Gnotobiotic Mouse Studies. All mouse experiments were approved by the Montana State University Institutional Animal Care and Use Committee. This study included humane endpoints as defined by an IACUC-approved list of criteria (see Supplementary Information) to maximize consistency of observations while minimizing the need for the experimental endpoint of death. All studies were conducted with attending veterinarian oversight. C57BL/6 mice were bred and maintained at the Montana State University Animal Resource Center, an American Association for the Accreditation of Laboratory Animal Care accredited facility. Germ-free mice were housed in hermetically sealed and Hepa-filter ventilated, vinyl isolators and received autoclaved water and food (LabDiet, St. Louis, Missouri). LabDiet® mouse chow (Land-O-Lakes, Inc) was used in all experiments, and lab deionized water was used as the water source. All food and water for germ-free mice was autoclaved, and then quarantined and tested for contamination prior to use.

C57BL/6 mice deficient for the murine *as3mt* gene (As3mt-KO) were used as previously described (Coryell *et al.*, 2018). Breeding pairs of As3mt-KO mice were originally obtained from Drs. Lora L. Arnold and Samuel M. Cohen (University of Nebraska Medical Center) and Drs. Christelle Douillet and Mirek Styblo (University of North Carolina), and used to establish a breeding colony at Montana State University. These mice were originally derived at the US Environmental Protection Agency as described previously (Drobna *et al.*, 2009). Germ-free status was monitored regularly by attempting aerobic and anaerobic culture techniques on rich medium (Mueller-Hinton broth and agar plates) and by periodic PCRs targeting the bacterial 16S rRNA encoding gene with DNA extracted from stool serving as template.

For introducing bacterial strains into mice, overnight cultures of *E. coli* AW3110 or AW3110::*fmt* were collected by centrifugation (8000 x g) and washed 3× with phosphate buffered saline (PBS, 100 mM K_2PO_4, 0.85% NaCl, pH 7.2). Cells were suspended in PBS and 100 μL of this slurry was used to inoculate germ-free mice via oral gavage (~10^9 CFU per mouse). Colonization was confirmed by direct plating from stool onto LB agar and retention of genomic *fmt* was verified in AW3110::*fmt* by PCR using *fmt*-specific primers (Supplementary Table 1).

All arsenic exposures were as As^{III}. For low-level exposure, C57BL/6 mice were exposed to 2.5 ppm As^{III} in drinking water *ad libitum*. After 28 days of exposure, mice were humanly euthanized in accordance with current guidelines by isoflurane overdose and tissues were collected for arsenic quantification. For high-level, lethal exposures, C57BL/6 As3mt-KO mice were exposed to 20 ppm As^{III} in drinking water *ad libitum*. The experiment continued until lethality or mice reached a veterinary guided humane endpoint determined by a combination of observed changes (ie, >15% weight loss, dehydration, ruffed fur, moribund, and lethargy) at which point they were humanely euthanized. For all experiments, daily fecal pellets were collected and frozen at –80°C for RNA extraction or quantification of total arsenic.

Arsenic Quantification. Arsenic concentrations in mouse biological samples were determined using an Agilent 1260 ICP-MS, using arsenic(III) oxide (Sigma-Aldrich, 99.995% trace metals basis) as the standard. Mouse tissue and fecal pellet samples were weighed and digested in a 70% solution of trace metal grade nitric acid (VWR International, Radner, PA) using heat and pressure (115°C, 29.7 PSI for 30 min). Digested samples were diluted in ultra-pure water to achieve a final nitric acid concentration of 5%. These dilutions were centrifuged at 2500 rpm for 10 min to remove any particulates and the supernatants collected for analysis. Samples were injected via a constant-flow-rate peristaltic auto-sampler and the results quantified against an external standard curve using the Agilent's ChemStation software package.

In Vivo Gene Expression Analysis. Groups of 2–5 mice were co-housed in the same cage during exposure studies. Fecal pellets were collected by holding mice above the cage and collecting pellets directly into sterile Eppendorf tubes. Fecal pellets collected for RNA extraction were immersed into RNA later (Invitrogen, Vilnius, and Lithuania), and RNA was extracted using the RNeasy® Mini Kit (Qiagen, Hilden, Germany) and stored at –80°C.

After determining the concentration of RNA by spectrophotometry (NanoDrop 2000, Thermo), 250 ng total RNA was reverse transcribed into cDNA with iScript™ Reverse Transcription Supermix for RT-PCR (Bio-RAD, Hercules). The resulting cDNA was diluted 5-fold for qPCR analysis using AzuraQuant™ Green Fast qPCR Master Mix (Azura Genomics Inc.) with primers listed (Antonopoulos *et al.*, 2009; Chern *et al.*, 2011) in Supplementary Table 1. qPCRs were performed in triplicate using a LightCycler®

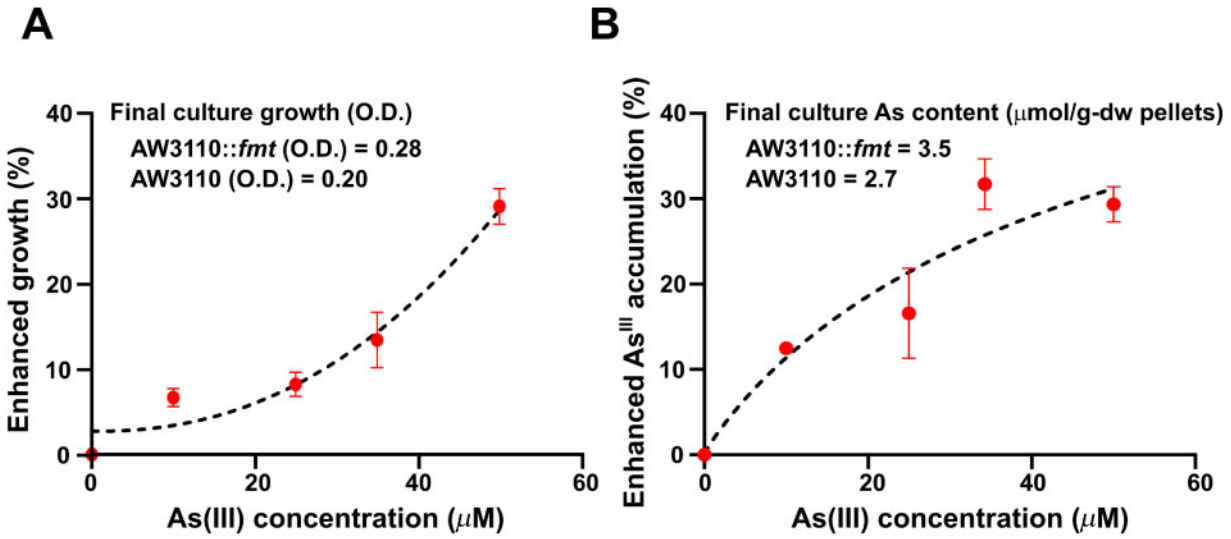

Figure 2. Growth and As^{III} bioaccumulation of AW3110 and AW3110::*fmt*. (A) The percent enhanced culture growth of AW3110::*fmt* relative to AW3110 with increasing media As^{III} concentration. (B) The percent enhanced As^{III} accumulation in AW3110::*fmt* relative to AW3110 with increasing As^{III} concentration. All experiments were performed in triplicate. Error bars represent the standard deviation of the mean.

96 thermocycler (Roche) as described above. Raw data were analyzed with LightCycler® 96 Application Software Version 1.1 (Roche) and gene expression was evaluated using the $2^{-\Delta\Delta CT}$ method.

In Vivo and In Vitro Protein Analysis. Fecal samples were collected directly from mice and stored at –80°C before analysis. Fecal pellets were cut on dry ice, weighed, and suspended in 500 μL PBS containing 5% protease inhibitors (Roche). Pellets (0.5 g) were first manually homogenized with a pipette tip and vigorous vortexing. Disrupted pellets were centrifuged (250 rpm, 5 min) to pellet insoluble material, followed by centrifuging the supernatant (8000 rpm, 15 min, 4°C) to collect bacterial cells. The resulting pellets were washed 3× in 500 μL PBS containing 5% protease inhibitors, followed by lysis with ultra-sonication on ice. For *in vitro* work, overnight bacterial cultures were collected by centrifugation (8000 rpm, 5 min, 4°C), washed 3× in PBS, resuspended in PBS containing 1% protease inhibitors, and also lysed by ultra-sonication on ice.

Protein concentrations of all samples were determined by Pierce™ BCA Protein Assay Kit (ThermoFisher). Samples containing 10, 5, 2.5, 1.25, or 0.625 ng of total protein were directly spotted onto a polyvinylidene difluoride (PVDF) membrane, washed 3× in tris-buffered saline containing 1% Tween 20 (TBST) and blocked with 5% skim milk in TBST for 1 h. Following 3× washes in TBST, membranes were incubated in block solution (1:2000 dilution) containing either His-tag antibody coupled to horseradish peroxidase (HRP) or antibodies raised against glyceraldehyde-3-phosphate dehydrogenase (GAPDH) coupled to HRP. Membranes were finally washed 3× for 15 min each with TBST, then blots visualized by SuperSignal™ West Pico PLUS Chemiluminescent Substrate (Invitrogen).

Statistical Analyses. Growth differences between *E. coli* strains, bioaccumulation of arsenic during exposure (*in vitro* and *in vivo*), and CFU per dry gram weight of mouse pellets (*in vivo*) were evaluated temporally using 2-way repeated measures ANOVA. Total arsenic in organs was examined using regular 2-way ANOVA with *p*-value correction for multiple comparisons. All ANOVAs were performed in GraphPad Prism (La Jolla, CA). Mouse survival between groups during arsenic exposure was compared using the Mantel-Cox test (GraphPad Prism).

RESULTS

Construction and In Vitro Characterization of *E. coli* AW3110::*fmt*

Fmt is a 67 amino acid peptide with a predicted stoichiometry of at least 5As^{III} : 1Fmt (Merrifield *et al.*, 2004), deriving from 16 Cys residues (Figure 1) that are specific and strong targets for As^{III} binding. A synthesized *fmt* construct was subcloned as a PacI-AvrII restriction fragment into pGRG25, which facilitates convenient markerless insertion of transgenes into the *E. coli* chromosome followed by incubation at non-permissive temperatures (42°C) to eliminate the delivery plasmid and select for the *fmt* recombinant (McKenzie and Craig, 2006). Stable chromosome integration between *glmS* and *pstS* (Figure 1) was verified with diagnostic PCR. The insertion was upstream of *pstS*, which is essential for normal regulation of the phosphate stress response (PSR) operon. Since the PSR is global in nature (Hsieh and Wanner, 2010), it was important to rule out potential polar effects on *pstS* expression in AW3110::*fmt* (i.e., equivalent to silencing PstS), which would complicate interpretations of AW3110::*fmt* effects *in vitro* and *in vivo*. Lack of PstS would be expected to yield constitutive expression of AP. However, a normal PSR was observed in both strains wherein AP activity induced within 0.5 hours after cells were suspended in zero phosphate media (Supplementary Figure 1, $p = 0.429$), leading us to conclude that with the exception of Fmt effects, the AW3110::*fmt* would be functionally isogenic compared to AW3110.

Subsequent characterization then compared AW3110::*fmt* and AW3110 for growth response and As^{III} accumulation. Incubation in LB broth containing increasing levels of As^{III} illustrated that the recombinant strain grew better (Figure 2A) and accumulated more arsenic (Figure 2B) than the parental AW3110. Growth was identical in the absence of As^{III}, but the capacity to sequester As^{III} was apparently advantageous as increasing As^{III} progressively enhanced the growth differential

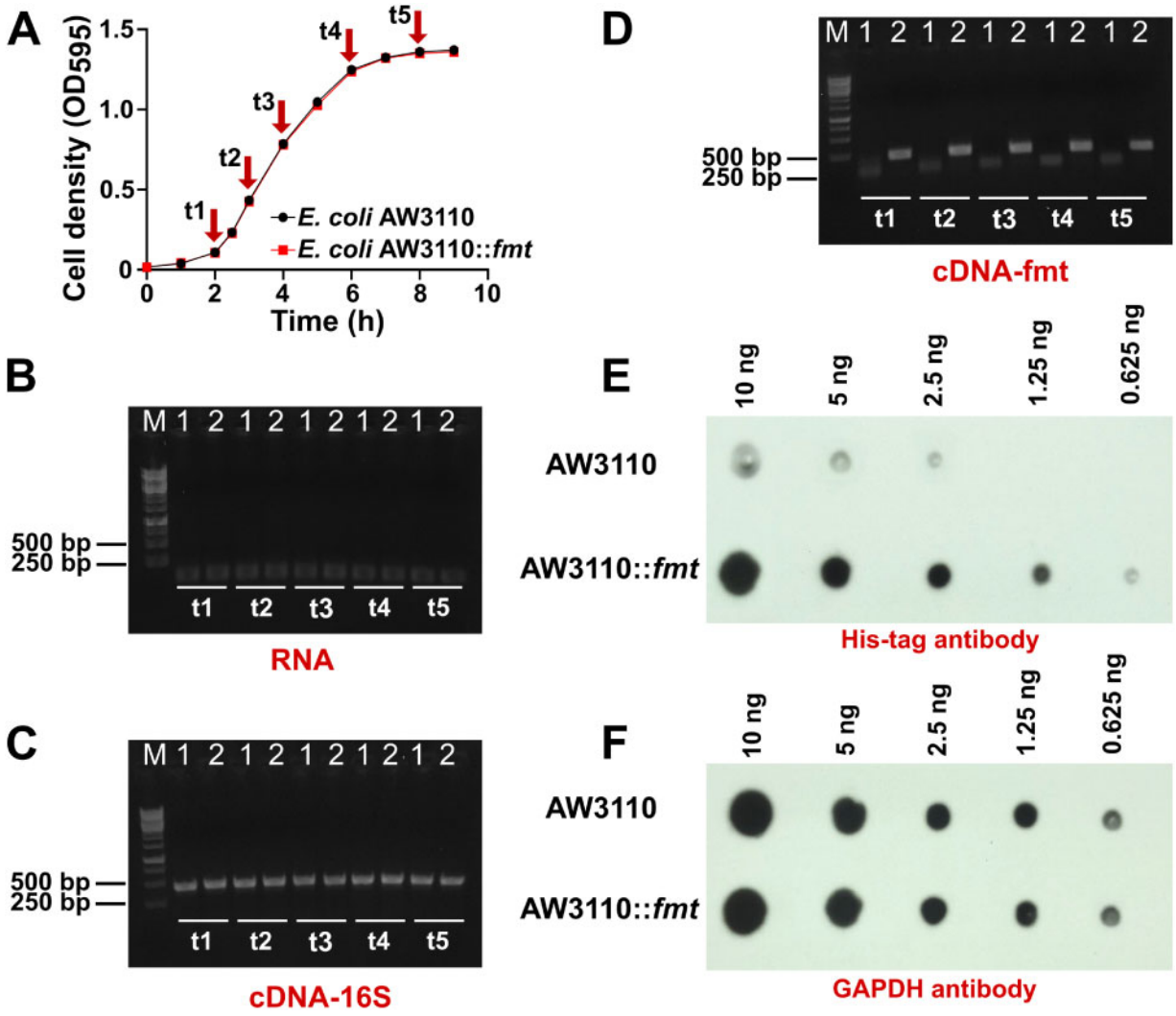

Figure 3. Verification of constitutive transcription of *fmt* and Fmt stability in AW3110::*fmt* cultures. Lane assignments in panels A–D: (1) AW3110; (2) AW3110::*fmt*. (A) Identical culture growth profiles of AW3110 and AW3110::*fmt* in LB broth without As^{III}. (B) Lack of PCR amplicons in purified and DNAse-treated RNA preparations verifying lack of amplifiable DNA. (C) Identical 16S rRNA gene RT-PCR profiles of both strains during growth. (D) Presence of *fmt* RT-PCR amplicons in AW3110::*fmt* and absence in the control strain AW3110. (E) Western dot blots illustrating Fmt peptide presence and stability in AW3110::*fmt* and background His-tag binding in control cell extracts. (F) Western dot blots of the positive control protein GAPDH in both strains.

between these strains (Figure 2A). The As^{III} accumulation response was curvilinear, suggesting Fmt sequestration was saturable (Figure 2B), as would be expected. The enhanced growth of AW3110::*fmt* monoculture in the presence of As^{III} also suggested AW3110::*fmt* would be more competitive. This was verified in co-culture experiments, wherein both strains were inoculated at equal proportion and then tracked over the course of three sub-cultures. AW3110 and AW3110::*fmt* maintained their original proportions in the absence of As^{III} (~50% each), but AW3110::*fmt* quickly dominated in As^{III} media (~75%, Supplementary Figure 2). We note that even though Fmt provided a reproducible fitness advantage, the impact was not large enough to exclude the wild-type strain. This result suggests that energy costs involved with constitutive production of the peptide (i.e., energy required) did not overcome the benefit of production (fitness advantage).

RT-qPCR verified constitutive *fmt* expression (Figs. 3A–D), thereby establishing a link between gene transcription and cell response to As^{III} exposure. Additional experiments then verified the presence and the stability of the encoded protein (Figs. 3E–F). Some faint background binding of the His-tag antibody occurred in the control strain, but nevertheless there was a clear distinction relative to the recombinant strain AW3110::*fmt* (Figure 3E). By contrast, there was no discernable difference between these strains with respect to the detection of the positive control (housekeeping) protein, GAPDH (Figure 3F).

Characterization of *E. coli* AW3110::*fmt* in Gnotobiotic Mice

The above pure culture assessments provided sufficient evidence to advance the study to examine potential As^{III} bioaccumulation function and importance in the mouse gut environment. Both *E. coli* strains were gavaged separately into groups of germ-free, C57BL/6 mice and allowed to colonize unperturbed until CFU/g stool was stable (~2 weeks). Mice were then exposed to a low level of As^{III} (2.5 ppm) *ad libitum* in drinking water. The water consumption was recorded every day, and no significant difference were observed between gnotobiotic

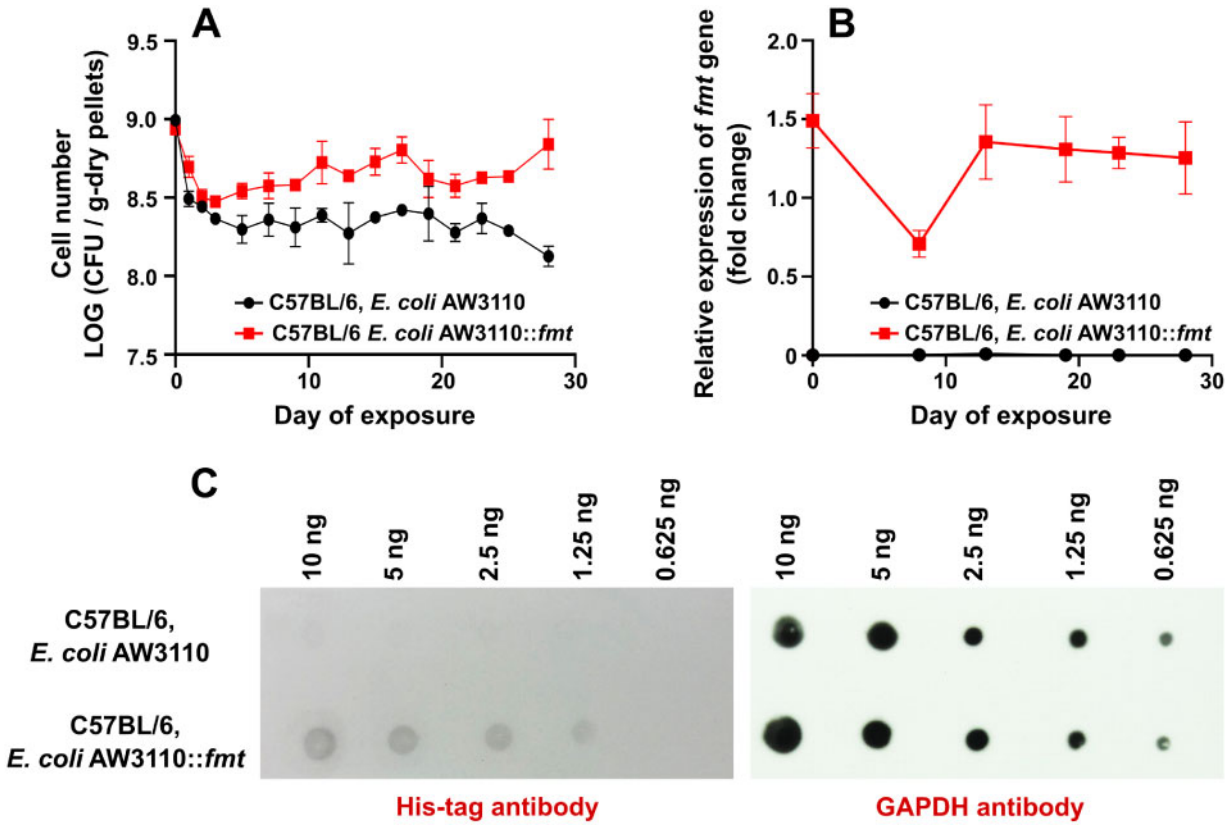

Figure 4. *E. coli* colonization and verification of constitutive *in vivo fmt* transcription and Fmt stability. (A) Colonization and viability as measured by CFU in stool. Results based on two independent experiments of n = 3 replicates per experiment. AW3110::*fmt* comprised significantly greater CFU/g-dry stool pellet compared to AW3110 (2-way repeated measures ANOVA, $p = .0141$, df = 1). Error bars represent standard deviation of the mean. (B) Expression of *fmt* relative 23S rRNA encoding gene as determined by RT-qPCR of RNA extracted from stool pellets over the course of exposure to 2.5 ppm As^{III}. Results based on two independent experiments of n = 3 replicates per experiment. Error bars represent standard deviation of the mean. (C) Presence of Fmt in stool of AW3110::*fmt* colonized mice and absence in AW3110 control mice, as compared to comparable levels of GAPDH (positive control protein) in all mice.

AW3110 mice and gnotobiotic AW3110::*fmt* mice (Supplementary Figure 3, $p = 0.540$). *E. coli* viability/survival was examined via agar plate counts derived from serially diluted homogenized mouse stool pellets. *E. coli* CFU in stool from both mouse treatment groups initially declined following introduction of As^{III}, but thereafter stabilized for both strains (Figure 4A). As with LB-cultured cells, the AW3110::*fmt* recombinant strain exhibited significantly enhanced As^{III} tolerance as indicated by significantly greater CFU throughout the exposure (Figure 4A, $p = 0.014$). Analysis of RNA extracted from stool pellets confirmed constitutive *fmt* expression (Figure 4B) as well as Fmt presence and stability in total protein extracted from AW3110::*fmt* only microbiomes (Figure 4C). Collectively, the results of these experiments indicated that *in vivo* behavior and function differences between the *E. coli* strains were quite similar to that observed in LB culture.

Parallel experiments were conducted to quantify the degree to which microbiome Fmt protected mice from ingested As^{III}. Given evidence of enhanced bioaccumulation by AW3110::*fmt* (Figure 2B) and the higher gut microbial load in stool (Figure 4A), the expectation was that this might translate to the increased arsenic content in stool. Although variable at some collection time points, this was found to be the case; i.e., total stool arsenic in AW3110::*fmt* treated mice was significantly greater ($p = 0.001$) than from mice carrying the control strain (Figure 5A). And, increased arsenic excretion was accompanied by significantly reduced arsenic accumulation in all mouse organs/tissues examined (Figure 5B, $p < 0.0001$). Indeed, arsenic was significantly decreased in kidney ($p < 0.0001$) and colon ($p = 0.0240$), and below detection in spleen and lung of AW3110::*fmt* treated mice (Figure 5B). The final experiment examined whether reduced exposure and increased elimination of As^{III} would protect mice from lethal levels of acute arsenic exposure (20 ppm). Our previous study showed this mouse line was hypersensitive to arsenic and thus could be more readily used for acute toxicity assessments (Coryell *et al.*, 2018). Over the course of a replicated 20-day exposure trial (total n = 16 mice per treatments, 8 mice per replicate), mortality was greater ($p = 0.007$) in mice colonized by the control strain, AW3110 (Figure 6). Reduced mortality observed in AW3110::*fmt* mice is conceptually and physiologically consistent with reduced exposure (Figure 5).

DISCUSSION

In the current study, we examined the specific question, "Does microbiome arsenic bioaccumulation influences host exposure and mortality when ingesting the toxicant, As^{III}?". While quite basic in nature, this rather simple question also reflects current understanding of gut microbiome-arsenic interactions; i.e., there exists very little information that provides even the most rudimentary understanding of how the gut microbiome affects arsenic fate and transport in the gut environment. Recent studies of arsenic treatment of wild type mice reported significant perturbation of microbiome taxonomic structure and

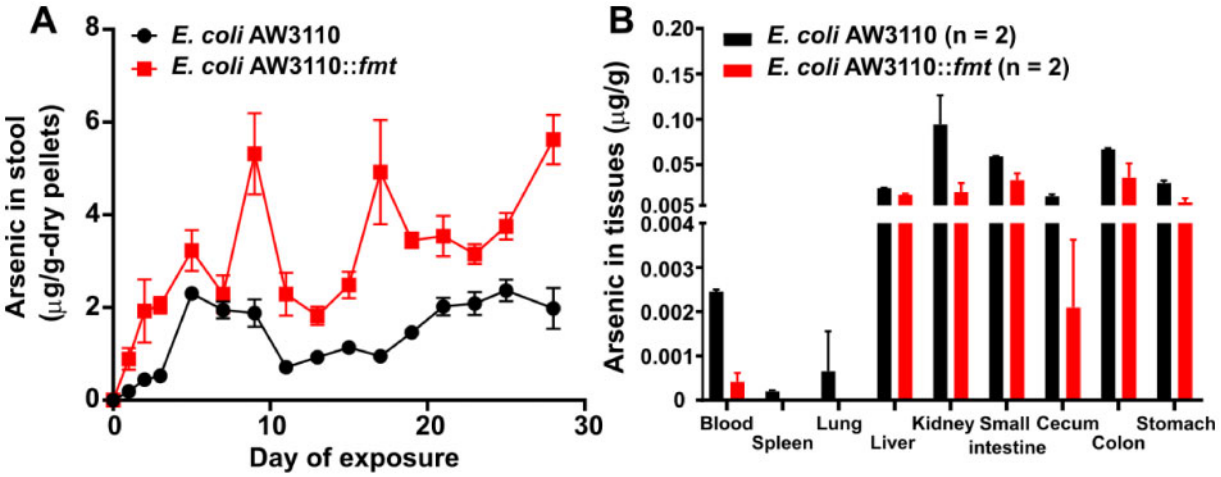

Figure 5. Mouse arsenic accumulation as influenced by microbiome expression of a functional Fmt. (A) Total arsenic content in mouse stool pellets. AW3110::*fmt* bioaccumulated significantly more arsenic compared to AW3110 during low-level (2.5 ppm) As^{III} exposure (2-way repeated measures ANOVA, $p = .001$, df = 1). Results based on two independent experiments of n = 3 replicates per experiment. (B) Total arsenic in organs of gnotobiotic mice following 28 days of exposure to 2.5 ppm As^{III} in drinking water. Overall, gnotobiotic mice colonized with AW3110::*fmt* accumulated less total arsenic in organs (2-way ANOVA, $p < .0001$, df = 1). Pairwise comparisons of each organ revealed significantly lower arsenic in kidney ($p < .0001$) and colon ($p = .024$) upon *p*-value correction. No arsenic was detected in spleen and lung of gnotobiotic AW3110::*fmt* mice. Error bars represent the standard deviation of the mean.

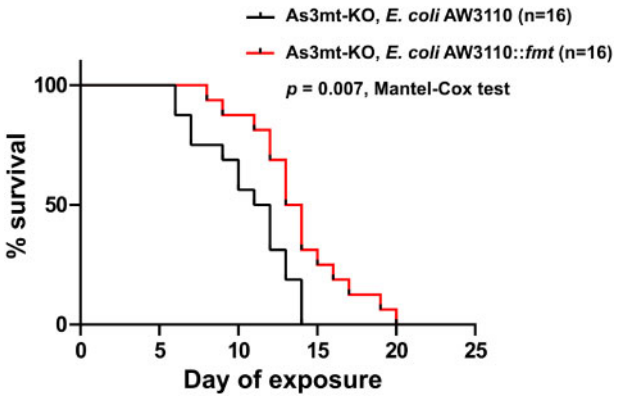

Figure 6. Survival of gnotobiotic, As3mt-KO mice following high-level (20 ppm) As^{III} exposure. Survival lines represent mortality in 2 replicate experiments (8 mice per group) with AW3110 and AW3110::*fmt* colonized mice. Mice colonized with AW3110::*fmt* survived significantly longer than mice colonized with AW3110 (Mantel-Cox test, $p = .007$).

metabolism (Guo *et al.*, 2014; Liu *et al.*, 2019; Lu *et al.*, 2014; Richardson *et al.*, 2018). We regard these as important foundational studies, but also point to the need to understand microbiome functions and reactions at a more detailed level. Other studies demonstrated that murine or human gut microbiome samples reduced As^{V} and/or methylate As^{III} (Hall *et al.*, 1997; Rowland and Davies, 1981), but these were *ex vivo* enrichment incubations that demonstrated metabolic *potential* but not actual gene expression or *in situ* function in the gut. Likewise, documented occurrence of specific functional genes in the human gut microbiome (i.e., stool metagenomes) (McDermott *et al.*, 2020) also does not prove functional relevance. So, while such studies provide strong evidence that microbiomes can *potentially* influence arsenic toxicity, direct experimental evidence of overall impact on host exposure is lacking. In the current study, the use of genetically customized gut microbiomes with gnotobiotic mice serves to bridge this gap.

Our prior efforts with germ-free and humanized mice definitively demonstrated that an intact microbiome protects the host from arsenic toxicity (Coryell *et al.*, 2018); arsenic excretion was significantly altered, at least suggesting the microbiome may contribute to host protection via arsenic bioaccumulation (Coryell *et al.*, 2018). However, an intact mammalian gut microbiome potentially will have a broad range of arsenic transformation or trafficking functions (Coryell *et al.*, 2019; McDermott *et al.*, 2020) and thus it is difficult to link specific microbiome activities with specific outcomes. In the current study, we deliberately selected a reductionist approach that exerted strong controls over microbiome-arsenic interactions. Specifically, *E. coli* AW3110 was used because it is an △*arsRBC* mutant and the *arsM* gene is absent, thus lacks the ability to reduce As^{V} to As^{III} (*arsC*) or to actively excrete As^{III} (*arsB*) or to methylate As^{III} (Carlin *et al.*, 1995). This mutation renders this strain more sensitive to As^{III} (Carlin *et al.*, 1995), but also offers a "clean" genetic background with respect to potential microbiome arsenic reduction-oxidation transformations or efflux. In the acute toxicity experiments, As3mt-KO mice were used because they could significantly prolong retention of inorganic arsenic in tissues and affect the clearance of arsenic (Hughes *et al.*, 2010). Within this background, we were able to manipulate the ability to bioaccumulate As^{III} with a single gene and thus directly address the relative importance of this singular microbiome function.

Microbial arsenic bioaccumulation may derive from several mechanisms. For example, recent studies illustrated As^{V} incorporation into microbial lipids (i.e., arsenolipids) (Pandey and Bhatt, 2015; Takeuchi *et al.*, 2007; Wang *et al.*, 2018). Another mechanism involves arsenic binding to proteins (Shen *et al.*, 2013) due to the strong attraction of trivalent arsenicals for sulfhydryl groups (Shen *et al.*, 2013) (e.g., As^{III}, as used here). A well characterized example of this arsenic-protein interaction involves the ArsR protein (Páez-Espino *et al.*, 2009), which has been shown to increase arsenic bioaccumulation when expressed from a multicopy plasmid platform (Ke *et al.*, 2018). It is not reasonable to entirely discount this type mechanism in the current study, however, the ArsR specific mechanism would

not play a role because the ArsR protein *per se* is absent in AW3110. A third mechanism that is of direct relevance to the current study again involves As^{III}-sulfhydryl interactions as found in metallothioneins (MTs). MTs are ubiquitous in nature and have been found in mammals, plants, eukaryotic microorganisms, and many prokaryotes, such as *Cyanobacteria*, pseudomonads, α-*Proteobacteria*, γ-*Proteobacteria*, and *Firmicutes* (Blindauer, 2011; Klaassen *et al.*, 1999). Metagenomic sequencing of human samples (stool) suggests *fmt* presence in the *Firmicutes* and *Bacteroidetes* phyla, which constitute the primary reservoir in the human gut microbiome (Arumugam *et al.*, 2011). Currently, we cannot find any literature confirming MT expression in the gut, but the potential for bacterial expression is certainly present. The *F. vesiculosus* metallothionein (Fmt) used here will sequester As^{III} and thus reduces inactivation of critical cellular processes that involve sulfhydryl-containing proteins. This protective function resulted in enhanced growth in As^{III}-containing environments (Figure 2), similar to enhanced copper and cadmium resistance associated with a range of soil metallothioneins just recently characterized by Li *et al.* (2020).

Fmt was previously used as a plasmid-borne maltose binding protein fusion in conjunction with a GlpF aquaglycerol porin (to enhance As^{III} uptake) in *E. coli* to demonstrate a potential bioremediation tool for ppb level arsenic contamination levels (Singh *et al.*, 2008). In the current study, we elected to express the Fmt peptide from a single copy, genome encoded gene to more reasonably represent copy number expression in the mouse gut, as well as to eliminate potential *in vivo* plasmid loss or fitness costs inherent with plasmid maintenance in the gut. As such, Fmt again demonstrated the capacity to increase As^{III} bioaccumulation *in vitro* (Figure 2B) and presumably *in vivo* as indicated by increased arsenic levels in stool samples (Figure 5A). Furthermore, mouse mortality was reduced and arsenic loads were significantly reduced in kidney, lung, colon, and spleen, which was previously shown by our group to differ in arsenic accumulation when the microbiome was altered/perturbed (Coryell *et al.*, 2018, Figures 5B and 6). Though we did not fully account for possible accumulation or excretion routes, our results provide definitive evidence that the same strategy is relevant to mammalian health, just as microbial bioaccumulation has been suggested to represent an environmental bioremediation strategy, emphasizing removal and sequestration (Páez-Espino *et al.*, 2009). With minimal conceptual extension, this could be viewed similarly in the context of the gut as an important prophylactic and/or probiotic intervention in highly exposed populations. Indeed, results from this study are consistent with a probiotic study in Tanzania where a dietary supplement (yogurt enriched with *Lactobacillus rhamnosus*) reduced arsenic and mercury body burden in pregnant women (Bisanz *et al.*, 2014).

When examining Fmt stability *in vivo*, we met with unanticipated issues concerning degradation of the target protein via proteases, a problem we have not yet found described in the pertinent literature. Compared to all the organs, the gut contains the highest levels of endogenous and exogenous proteases (Antalis *et al.*, 2007) that likely decreased our ability to detect the His-tagged Fmt protein, and to a lesser extent the non-tagged GAPDH protein. Host protease activity was at least partially constrained by using very high levels (5%) of a protease inhibitor cocktail and repeated washing of the stool *E. coli* cells prior to lysis. This is noteworthy as few, if any, studies report problematic protein detection from mammalian stool or protocols that overcome these issues. Regardless, our optimized protocol reliably confirmed that Fmt was present in AW3110::*fmt*-colonized but not AW3110-colonized mice (Figure 4C).

Finally, we draw attention to a more fundamental concepts borne out by this study. Specifically, when considered in total, our results illustrate that expression of a single gene within a background microbiome composed entirely of *E. coli* (~5000 genes) and in the presence of 25,059 host (mouse) genes had a profound effect on the outcome of arsenic exposure. Further, enhanced As^{III} resistance and competitiveness by AW3110::*fmt* (Figure 2 and Supplementary Figure 2) assists in interpreting how and why arsenic treatments significantly perturbs gut microbiome composition, resulting in an imbalance of some taxa (dysbiosis) (Guo *et al.*, 2014; Lu *et al.*, 2014); i.e., enhanced As^{III} resistance leads to enhanced competitiveness and enhanced relative abundance. Taken together, this constitutes the first example of a specifically defined microbiome function that can be traced to a single gene and that confers a significant benefit to a mammalian host against an important environmental toxicant.

SUPPLEMENTARY DATA

Supplementary data are available at *Toxicological Sciences* online.

DECLARATION OF CONFLICTING INTERESTS

The author(s) declared no potential conflicts of interest with respect to the research, authorship, and/or publication of this article.

ACKNOWLEDGMENTS

The content is solely the responsibility of the authors and does not necessarily represent the official views of the National Institutes of Health.

FUNDING

Research reported in this publication was supported primarily by the National Cancer Institute of the National Institutes of Health under Award Number R01CA215784. T.R.M. also acknowledges support from the Montana Agricultural Experiment Station (Project 911310).

REFERENCES

Antalis, T. M., Shea-Donohue, T., Vogel, S. N., Sears, C., and Fasano, A. (2007). Mechanisms of disease: protease functions in intestinal mucosal pathobiology. *Nat. Clin. Pract. Gastroenterol. Hepatol.* **4**, 393–402.

Antonopoulos, D. A., Huse, S. M., Morrison, H. G., Schmidt, T. M., Sogin, M. L., and Young, V. B. (2009). Reproducible community dynamics of the gastrointestinal microbiota following antibiotic perturbation. *Infect. Immun.* **77**, 2367–2375.

Arumugam, M., Raes, J., Pelletier, E., Le Paslier, D., Yamada, T., Mende, D. R., Fernandes, G. R., Tap, J., Bruls, T., Batto, J.-M., MetaHIT Consortium., *et al.* (2011). Enterotypes of the human gut microbiome. *Nature* **473**, 174–180.

Agency for Toxic Substances and Disease Registry (ATSDR) Substance Priority List (SPL). (2019). Division of Toxicology and Human Health Sciences, Atlanta, GA. Available at: https://www.atsdr.cdc.gov/spl/index.html. Accessed February 13, 2021.

Bhattacharjee, P., Chatterjee, D., Singh, K. K., and Giri, A. K. (2013). Systems biology approaches to evaluate arsenic toxicity and carcinogenicity: an overview. *Int. J. Hyg. Environ. Health* **216**, 574–586.

Bisanz, J. E., Enos, M. K., Mwanga, J. R., Changalucha, J., Burton, J. P., Gloor, G. B., and Reid, G. (2014). Randomized open-label pilot study of the influence of probiotics and the gut microbiome on toxic metal levels in tanzanian pregnant women and school children. *mBio* **5**, e01580-01514.

Blindauer, C. A. (2011). Bacterial metallothioneins: past, present, and questions for the future. *J. Biol. Inorg. Chem.* **16**, 1011–1024.

Botero, L. M., Al-Niemi, T. S., and McDermott, T. R. (2000). Characterization of two inducible phosphate transport systems in rhizobium tropici. *Appl. Environ. Microbiol.* **66**, 15–22.

Carlin, A., Shi, W., Dey, S., and Rosen, B. P. (1995). The ARS operon of *Escherichia coli* confers arsenical and antimonial resistance. *J. Bacteriol.* **177**, 981–986.

Chern, E. C., Siefring, S., Paar, J., Doolittle, M., and Haugland, R. A. (2011). Comparison of quantitative PCR assays for *Escherichia coli* targeting ribosomal RNA and single copy genes. *Lett. Appl. Microbiol.* **52**, 298–306.

Coryell, M., McAlpine, M., Pinkham, N. V., McDermott, T. R., and Walk, S. T. (2018). The gut microbiome is required for full protection against acute arsenic toxicity in mouse models. *Nat. Commun.* **9**, 5424.

Coryell, M., Roggenbeck, B. A., and Walk, S. T. (2019). The human gut microbiome's influence on arsenic toxicity. *Curr. Pharmacol. Rep.* **5**, 491–504.

Cubadda, F., D'Amato, M., Mancini, F. R., Aureli, F., Raggi, A., Busani, L., and Mantovani, A. (2015). Assessing human exposure to inorganic arsenic in high-arsenic areas of latium: a biomonitoring study integrated with indicators of dietary intake. *Ann. Ig.* **27**, 39–51.

Drobna, Z., Naranmandura, H., Kubachka, K. M., Edwards, B. C., Herbin-Davis, K., Styblo, M., Le, X. C., Creed, J. T., Maeda, N., Hughes, M. F., *et al.* (2009). Disruption of the arsenic (+3 oxidation state) methyltransferase gene in the mouse alters the phenotype for methylation of arsenic and affects distribution and retention of orally administered arsenate. *Chem. Res. Toxicol.* **22**, 1713–1720.

Faita, F., Cori, L., Bianchi, F., and Andreassi, M. G. (2013). Arsenic-induced genotoxicity and genetic susceptibility to arsenic-related pathologies. *Int. J. Environ. Res. Public Health* **10**, 1527–1546.

Guo, X., Liu, S., Wang, Z., Zhang, X. X., Li, M., and Wu, B. (2014). Metagenomic profiles and antibiotic resistance genes in gut microbiota of mice exposed to arsenic and iron. *Chemosphere* **112**, 1–8.

Hall, L. L., George, S. E., Kohan, M. J., Styblo, M., and Thomas, D. J. (1997). In vitro methylation of inorganic arsenic in mouse intestinal cecum. *Toxicol. Appl. Pharmacol.* **147**, 101–109.

Hsieh, Y. J., and Wanner, B. L. (2010). Global regulation by the seven-component pi signaling system. *Curr. Opin. Microbiol.* **13**, 198–203.

Hughes, M. F., Edwards, B. C., Herbin-Davis, K. M., Saunders, J., Styblo, M., and Thomas, D. J. (2010). Arsenic (+3 oxidation state) methyltransferase genotype affects steady-state distribution and clearance of arsenic in arsenate-treated mice. *Toxicol. Appl. Pharmacol.* **249**, 217–223.

Ke, C., Zhao, C., Rensing, C., Yang, S., and Zhang, Y. (2018). Characterization of recombinant *E. coli* expressing arsr from rhodopseudomonas palustris cga009 that displays highly selective arsenic adsorption. *Appl. Microbiol. Biotechnol.* **102**, 6247–6255.

Klaassen, C. D., Liu, J., and Choudhuri, S. (1999). Metallothionein: an intracellular protein to protect against cadmium toxicity. *Annu. Rev. Pharmacol. Toxicol.* **39**, 267–294.

Li, X., Islam, M. M., Chen, L., Wang, L., and Zheng, X. (2020). Metagenomics-guided discovery of potential bacterial metallothionein genes from the soil microbiome that confer cu and/or cd resistance. *Appl. Environ. Microbiol.* **86**, e02907-19.

Liu, C. W., Chi, L., Tu, P., Xue, J., Ru, H., and Lu, K. (2019). Isobaric labeling quantitative metaproteomics for the study of gut microbiome response to arsenic. *J. Proteome Res.* **18**, 970–981.

Liu, J., Lu, Y., Wu, Q., Goyer, R. A., and Waalkes, M. P. (2008). Mineral arsenicals in traditional medicines: orpiment, realgar, and arsenolite. *J. Pharmacol. Exp. Ther.* **326**, 363–368.

Lu, K., Abo, R. P., Schlieper, K. A., Graffam, M. E., Levine, S., Wishnok, J. S., Swenberg, J. A., Tannenbaum, S. R., and Fox, J. G. (2014). Arsenic exposure perturbs the gut microbiome and its metabolic profile in mice: an integrated metagenomics and metabolomics analysis. *Environ. Health Perspect.* **122**, 284–291.

Maeda, M., Shimada, T., and Ishihama, A. (2015). Strength and regulation of seven rRNA promoters in *Escherichia coli*. *PLoS One* **10**, e0144697.

Martinson, J. N. V., and Walk, S. T. (2020). *Escherichia coli* residency in the gut of healthy human adults. *EcoSal Plus* **9**. doi:10.1128/ecosalplus.ESP-0003-2020.

McDermott, T. R., Stolz, J. F., and Oremland, R. S. (2020). Arsenic and the gastrointestinal tract microbiome. *Environ. Microbiol. Rep.* **12**, 136–159.

McKenzie, G. J., and Craig, N. L. (2006). Fast, easy and efficient: site-specific insertion of transgenes into enterobacterial chromosomes using tn7 without need for selection of the insertion event. *BMC Microbiol.* **6**, 39.

Merrifield, M. E., Ngu, T., and Stillman, M. J. (2004). Arsenic binding to *Fucus vesiculosus* metallothionein. *Biochem. Biophys. Res. Commun.* **324**, 127–132.

Morris, C. A., Nicolaus, B., Sampson, V., Harwood, J. L., and Kille, P. (1999). Identification and characterization of a recombinant metallothionein protein from a marine alga, *Fucus vesiculosus*. *Biochem. J.* **338**, 553–560.

Naujokas, M. F., Anderson, B., Ahsan, H., Aposhian, H. V., Graziano, J. H., Thompson, C., and Suk, W. A. (2013). The broad scope of health effects from chronic arsenic exposure: update on a worldwide public health problem. *Environ. Health Perspect.* **121**, 295–302.

Oremland, R. S., and Stolz, J. F. (2003). The ecology of arsenic. *Science* **300**, 939–944.

Oremland, R. S., and Stolz, J. F. (2005). Arsenic, microbes and contaminated aquifers. *Trends Microbiol.* **13**, 45–49.

Páez-Espino, D., Tamames, J., de Lorenzo, V., and Cánovas, D. (2009). Microbial responses to environmental arsenic. *Biometals* **22**, 117–130.

Pandey, N., and Bhatt, R. (2015). Arsenic resistance and accumulation by two bacteria isolated from a natural arsenic contaminated site. *J. Basic Microbiol.* **55**, 1275–1286.

Richardson, J. B., Dancy, B. C. R., Horton, C. L., Lee, Y. S., Madejczyk, M. S., Xu, Z. Z., Ackermann, G., Humphrey, G., Palacios, G., Knight, R., *et al.* (2018). Exposure to toxic metals triggers unique responses from the rat gut microbiota. *Sci. Rep.* **8**, 6578.

Rowland, I. R., and Davies, M. J. (1981). *In vitro* metabolism of inorganic arsenic by the gastro-intestinal microflora of the rat. *J. Appl. Toxicol.* **1**, 278–283.

Sambrook, J. 2001. *Molecular Cloning: A Laboratory Manual*, 3rd ed. Cold Spring Harbor Laboratory Press, Cold Spring Harbor, NY.

Shen, S., Li, X.-F., Cullen, W. R., Weinfeld, M., and Le, X. C. (2013). Arsenic binding to proteins. *Chem. Rev.* **113**, 7769–7792.

Singh, S., Mulchandani, A., and Chen, W. (2008). Highly selective and rapid arsenic removal by metabolically engineered *Escherichia coli* cells expressing *Fucus vesiculosus* metallothionein. *Appl. Environ. Microbiol.* **74**, 2924–2927.

Stolz, J. F., Basu, P., Santini, J. M., and Oremland, R. S. 2006. *Arsenic and Selenium in Microbial Metabolism*. pp. 107–130. Department of Biological Sciences, Duquesne University, Pittsburgh, PA 15282.

Stolz, J. F., and Oremland, R. S. (1999). Bacterial respiration of arsenic and selenium. *FEMS Microbiol. Rev.* **23**, 615–627.

Takeuchi, M., Kawahata, H., Gupta, L. P., Kita, N., Morishita, Y., Ono, Y., and Komai, T. (2007). Arsenic resistance and removal by marine and non-marine bacteria. *J. Biotechnol.* **127**, 434–442.

Wang, Q., Kang, Y. S., Alowaifeer, A., Shi, K., Fan, X., Wang, L., Jetter, J., Bothner, B., Wang, G., and McDermott, T. R. (2018). Phosphate starvation response controls genes required to synthesize the phosphate analog arsenate. *Environ. Microbiol.* **20**, 1782–1793.